Reports

Synthesis and Properties of Metallic Glasses That Contain Aluminum

Y. He, S. J. Poon, G. J. Shiflet

The synthesis and properties of a class of metallic glasses containing up to 90 atomic percent aluminum are reported. The unusual formability of the glasses and their structural features are pointed out. Mechanical properties including tensile fracture strength and Young's modulus are reported along with crystallization temperatures. The unusually high strengths of the aluminum glasses can be of significant importance in obtaining high-strength low-density materials.

During the search for aluminum-rich quasicrystals in the $Al_{20}Cr_2Ce$-type alloys [$Al_{18}Cr_2Mg_3$ structure, 184 atoms per unit cell (*1*)], a metallic glass (we refer to amorphous phases produced by rapid solidification) of composition $Al_{87}Fe_{8.7}Ce_{4.3}$ was observed (*2*). This unexpected finding of single-phase aluminum-rich glassy alloys produced in continuous ribbons has led to the synthesis of many more metallic glasses containing up to 90 atomic percent (at.%) aluminum, as to be discussed in this report.

The existence of amorphous metallic ribbons containing as much as 90 at.% aluminum has both scientific and technological implications. First of all, the unusual formability of these glassy phases is noted. For binary alloys of composition $A_{100-x}B_x$, it is generally observed that metallic glasses can only be formed when $85 > x > 15$ (*3*). In alloys containing more than two components, this result can be generalized. It is believed that this fact is related to the existence of a low eutectic region coinciding with the glass formation range. The eutectic region is favorable for the formation of metallic glasses because the liquid is stable to a lower temperature in this region than in other regions of the phase diagram. In principle, the degree of supercooling required to form a glass is reduced and crystallization is suppressed, thus rendering the formation of metallic glass possible (*4*). Quite different from the usual glass-forming systems, the liquidus temperatures of the related aluminum binary alloys reported here either increase or change little as the minority components are added to aluminum. Knowing these facts, one can say that the formation of glassy alloys based on 90 at.% aluminum is rather unique because there does not seem to be additional stability in the aluminum melt due to alloying. It should also be pointed out that the synthesis of amorphous aluminum is in itself a major challenge in materials physics. Although most simple metals and transition metals, when included with various amounts of gaseous impurities, can form amorphous phases easily as they are quench condensed onto cryogenic substrates, the formation of amorphous aluminum (or very aluminum-rich alloys) by quench condensation, which has a much higher cooling rate than rapid solidification, has not been observed (*5*). On the other hand, there were reports of amorphous aluminum alloys containing 70 to 80 at.% aluminum synthesized by ion beam mixing, ion implantation (*6*), and rapid solidification (*7*). These glassy samples were found to be brittle. In addition to their scientific novelty, the present alloys could have technological importance, especially in applications requiring high-strength low-density materials. This technological impact is expected, particularly in view of the well-established techniques in mass-producing metallic glass ribbons. In this report, some of the mechanical properties, stability, and structural features of these glassy aluminum alloys will be discussed.

With the formation of Al-Fe-Ce glassy alloys as the basis for obtaining other aluminum glasses, several dozen compositions were studied by replacing Fe with Co, Ni, and Rh; and Ce with other lanthanides, Y, and Hf in Al-Fe-Ce. Alloy ingots of compositions $Al_{90}(\alpha_{1-x}\beta_x)_{10}$ and $Al_{87}(\alpha_{1-x}\beta_x)_{13}$, where $0.3 < x < 0.7$; α = Fe; β = Y, La, Ce, Sm, Gd, Lu, and Hf; $Al_{87}Co_{8.7}Ce_{4.3}$, $Al_{87}Ni_{8.7}Ce_{4.3}$, $Al_{87}Rh_{8.7}Ce_{4.3}$, $Al_{87}Co_{8.7}Y_{4.3}$, $Al_{87}Co_{8.7}Hf_{4.3}$, $Al_{87}Ni_{8.7}Y_{4.3}$, and $Al_{87}Ni_{6.7}Hf_{6.3}$ were prepared by arc melting nominal amounts of elements in an argon atmosphere. Melt spinning was carried out in a partial helium atmosphere using a copper wheel (20 cm in diameter) with a typical circumferential velocity of 40 m/sec. Samples with compositions listed above were found to form single-phase metallic glasses. Their typical dimensions were 15 μm thick, 1 to 2 mm wide, and up to several meters long. The melt spun ribbons were very flexible and could easily be bent in half without fracturing. This bend test confirms the shear nature of the deformation process where long straight plastic shear steps are formed, which is consistent with other metallic glasses (*8*). Figure 1 is a scanning electron microscope (SEM) micrograph of a more complicated bending operation caused by perforation of the ribbon. Primary shear bands parallel to one another as well as secondary bands are visible and demonstrate that more complex deformation processes can be accommodated by the aluminum glass ribbon.

Using Cu K_α radiation, x-ray patterns show broad maxima near $2\theta = 38°$, followed by a second broad band near $2\theta = 70°$ (Fig. 2). This diffraction profile is typical of those of metallic glasses. The position and full width at half maximum of the first broad peak yield a nearest-neighbor distance of 2.86 Å, and an effective crystalline size of 11 Å, respectively. The limited spatial order is also characteristic of metallic glasses (*9*). Transmission electron microscopy further demonstrates that the glassy material does not contain small crystallites in

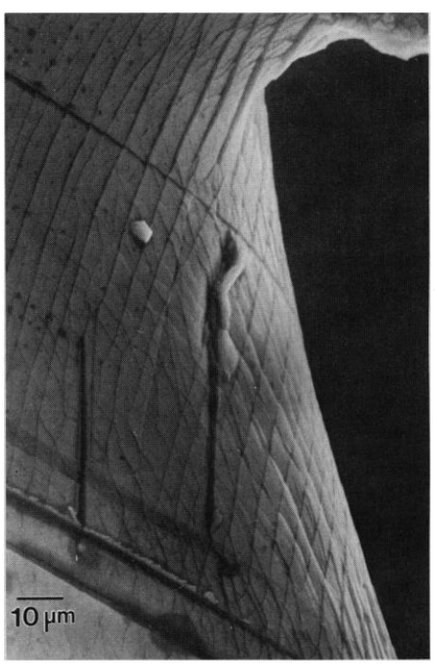

Fig. 1. Primary and secondary shear bands produced by complex bending (and perforation) of the $Al_{87}Fe_{6.7}Ce_{6.3}$ metallic glass ribbon in half. The steps are parallel to the bend axis.

Y. He and S. J. Poon, Department of Physics, University of Virginia, Charlottesville, VA 22901.
G. J. Shiflet, Department of Materials Science, University of Virginia, Charlottesville, VA 22901.

Table 1. Mechanical properties of aluminum glass materials.

Alloy	Tensile strength (MPa)	Young's modulus (GPa)	T_x (°C)
$Al_{90}Fe_5Ce_5$	940	66	250
$Al_{87}Fe_{8.7}Gd_{4.3}$	840	53	310
$Al_{87}Ni_{8.7}Ce_{4.3}$	500	46	300
$Al_{87}Ni_{8.7}Y_{4.3}$	880	50	260
$Al_{87}Co_{8.7}Ce_{4.3}$	790	63	300
$Al_{87}Co_{8.7}Y_{4.3}$	740	55	260
$Al_{87}Fe_{6.7}Ce_{6.3}$	670	59	300
$Al_{87}Rh_{8.7}Ce_{4.3}$	730	63	290

the matrix. The amorphous to crystalline transformation temperatures, T_x, for eight alloys are listed in Table 1. These temperatures are defined as the temperature where about 30 to 50% of the sample has transformed after being annealed for 5 minutes, as revealed by x-ray diffraction. Annealing experiments were carried out at 10°C increments, starting at 200°C. More detailed thermal analysis was performed on several samples by use of a differential scanning calorimeter (DSC, Perkin-Elmer 7 Series). The transformation temperatures determined by both methods are in agreement. Tensile strengths were tested at room temperature in an Instron machine with a strain rate of 1.3×10^{-4} sec^{-1}. Pneumatic grips with smooth surfaces were used to minimize deleterious gripping effects. Sample dimensions were measured in the SEM with a magnification calibration marker mounted near the samples. Following each test thicknesses were measured and fracture surfaces observed in the SEM.

The DSC result for $Al_{87}Fe_{8.7}Gd_{4.3}$ glass is shown in Fig. 3. It should be mentioned that the thermal stability and structural features of different $Al_{87}Fe_{8.7}Ln_{4.3}$ (Ln = lanthanide) are similar. X-ray measurements were carried out on samples that had been scanned to the three temperatures marked A, B, and C, and then cooled to ambient temperature. At point A, the diffraction pattern shows aluminum peaks and an amorphous band. The volume fraction of aluminum is estimated to be about 30%. At point B, the sample is found to contain mostly Al and an $Al_8Fe_{4-x}Gd_x$ phase ($Mn_{12}Th$ structure), as well as a trace amount of an $Al_2Fe_{1-x}Gd_x$ phase (Cu_2Mg structure). Phases obtained at point C are the same as those at point B. Thus, the first exothermic peak is attributable to the primary crystallization of aluminum in the glass, leaving behind an amorphous host that transforms at a higher temperature (second peak). The composition of this more stable glass is then different from the glassy host before crystallization takes place. The origin of the third exothermic peak, showing no apparent structural transformation, is not known at present. Repeating this study on $Al_{87}Fe_{6.7}Gd_{6.3}$ produces aluminum and an $Al_2Fe_{1-x}Gd_x$ phase of the Zn_2Mg structure as the major phases and a trace amount of $Al_8Fe_{4-x}Gd_x$ after the entire sample is crystallized.

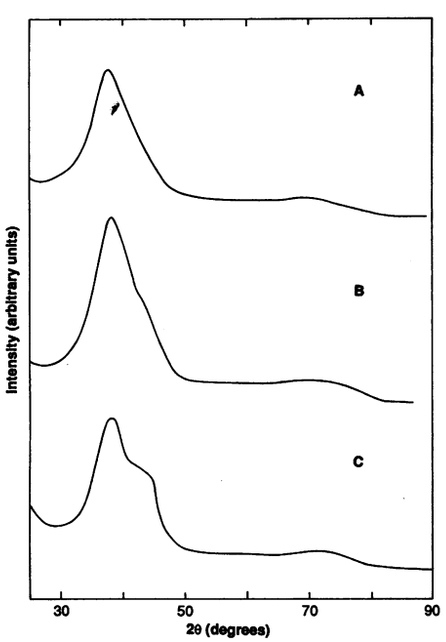

Fig. 2. X-ray diffraction traces of (A) $Al_{87}Fe_{6.7}Ce_{6.3}$, (B) $Al_{87}Fe_{8.7}Ce_{4.3}$, and (C) $Al_{87}Fe_{9.3}Ce_{3.7}$ metallic glasses.

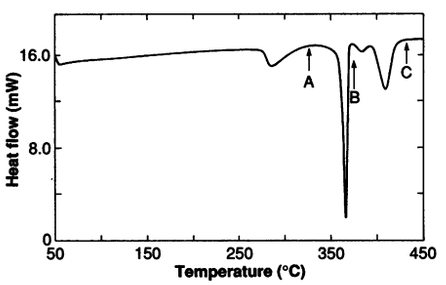

Fig. 3. Differential scanning calorimetry result for glassy $Al_{87}Fe_{8.7}Gd_{4.3}$.

X-ray profiles illustrating the structural trend in the Al-Fe-Ce alloys at increasing iron content are shown in Fig. 2. Replacing cerium by other lanthanides produces similar patterns. Although accurate structural information awaits detailed x-ray and neutron measurements and analyses, some special features noted in our qualitative scans are worth pointing out. These features, together with results from thermal analysis discussed above, could provide preliminary clues to the formation of glassy aluminum alloys. It is noticed that as the iron content is increased from $Al_{87}Fe_{6.7}Ce_{6.3}$ to $Al_{87}Fe_{9.3}Ce_{3.7}$, an additional shoulder structure emerges in the first peak (Fig. 2, b and c). This shoulder becomes so pronounced in the 9.3 at.% Fe alloy that the first broad peak now appears to constitute two amorphous bands. The position of this additional peak results in a near-neighbor distance of 2.55 Å. This distance is one of the typical near-neighbor distances in intermetallic compounds of the Al-Fe series. Considering the 2.86 Å Al-Al and 2.55 Å Al-Fe distances derived from the first "split" band, it might be tempting to suggest the existence of two amorphous phases, one containing almost pure aluminum and the other Al-Fe-Ce in the sample. This situation is very unlikely, however, because it is found that the crystallization temperature of aluminum glasses decreases rapidly when aluminum increases from 87 to 90 at.%. The existence of almost pure glassy aluminum on a macroscopic scale is thus unrealistic. The appearance of a shoulder structure is probably the result of some kind of short-range ordering of iron in the glass. Regarding the unusual formability of this class of metallic glasses, we conjecture that eutectic regions favoring metallic glassy phases might exist between aluminum and both the compounds $Al_8Fe_{4-x}Ce_x$ and $Al_2Fe_{1-x}Ce_x$. In light of the conventional theory of glass formation (*4*), growth of aluminum and these compounds is greatly suppressed even if nucleation can take place. The strong Al-Al and Al-Fe correla-

Fig. 4. Fracture surface of the $Al_{90}Fe_5Ce_5$ metallic glass.

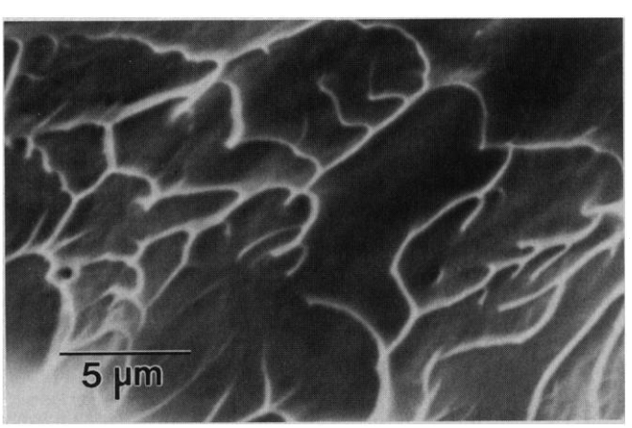

tions inferred from the "split" amorphous band and the mode of crystallization seems to be consistent with this picture. Although this simple model can account for easy glass-forming systems, its role in the present case should be viewed with caution because of the tremendous crystallization tendency of aluminum. Thus, the unusual formability of these glassy aluminum alloys deserves further studies.

High tensile strengths are expected, in general, for metallic glasses. Tensile fracture strengths of aluminum-based metallic glass ribbons are listed in Table 1. These strengths, in general, greatly exceed the strongest commercial aluminum alloys. For an aluminum alloy to achieve a strength of greater than 500 MPa, it must be highly developed and carefully thermally treated to peak strength. At a strength of 940 MPa the $Al_{90}Fe_5Ce_5$ alloy is the strongest we tested. The $Al_{87}Fe_{8.7}Gd_{4.3}$ and $Al_{87}Ni_{8.7}Y_{4.3}$ alloys have strengths near the Al-Fe-Ce material and, with modification of the ratio of elements, these values could undoubtedly be improved upon. When examined in SEM the fracture surfaces are fairly typical of metallic glass material. A typical fracture surface is shown in Fig. 4. This micrograph is of the $Al_{90}Fe_5Ce_5$ alloy and although not much ductility is observed (that is, no overall necking) the material does not fracture in a completely brittle fashion. The vein structure consists of protrusions on the fracture surfaces. These markings can be taken as evidence of local necking (*10*). We can describe the fracture of metallic glasses as "ductile" if it is a result of, at least locally, large plastic strains. In uniaxial tension, it occurs along the plane of the shear band. In tension, at relatively high stresses, metallic glasses deform extremely inhomogeneously. A large number of shear bands are visible within 20 μm below the fracture surface. Further examination of the ribbon failed to reveal any slip activity in areas other than near the fracture surface. Young's modulus data listed in Table 1 were determined from the elastic portion of the force versus displacement curve. Thirty-millimeter gauge sections were used and tested in a similar fashion as the tensile fracture tests. Several tests were run for each specimen. In general the material with the highest fracture strengths also showed the higher Young's modulus data. The modulus of the $Al_{90}Fe_5Ce_5$ metallic glass was the highest at 66 GPa. It is expected that the present class of alloys will receive much attention as potential high-strength, low-density materials. Although the current alloys discussed in this report have moduli lower than crystalline aluminum alloys, it is suggested that with further research the properties can be optimized.

REFERENCES AND NOTES

1. S. Samson, *Acta Crystallogr.* **11**, 851 (1958).
2. After our work was completed, we learned of an independent report of glassy phases in Al-Y-Ni, Al-Ni-Zr, Al-Hf-Ni, Al-Y-M, and Al-La-M (M = Fe, Co, Ni, Cu) alloys by A. Inoue, K. Ohtera, A. P. Tsai, T. Masumoto, *Jpn. J. Appl. Phys.* **27**, L479 (1988).
3. T. Egami and Y. Waseda, *J. Non-Cryst. Solids* **64**, 113 (1984).
4. F. Spaepen and D. Turnbull, *Annu. Rev. Phys. Chem.* **35**, 241 (1984).
5. H. A. Davies, in *Amorphous Metallic Alloys*, F. E. Luborsky, Ed. (Butterworths, Boston, 1983), pp. 8–25.
6. D. M. Follstaedt and S. T. Picraux, in *Alloy Phase Diagrams*, L. H. Bennett, B. C. Giessen, T. B. Massalski, Eds. (Materials Research Society, Pittsburgh, 1984), pp. 94–101; also J. A. Knapp and D. M. Follstaedt, *Phys. Rev. Lett.* **56**, 1827 (1986).
7. A. Inoue, A. Kitamura, T. Masumoto, *J. Mater. Sci.* **16**, 1895 (1981); R. O. Suzuki, Y. Komatsu, K. E. Kobayashi, P. H. Shingu, *ibid.* **18**, 1195 (1983).
8. H. J. Leamy, H. S. Chen, T. T. Wang, *Metall. Trans.* **3**, 699 (1972).
9. P. H. Gaskell, in *Glassy Metals II*, H. Beck and H. J. Guntherodt, Eds. (Springer-Verlag, New York, 1983), pp. 5–49.
10. F. Spaepen and A. I. Taub, (*4*), pp. 231–256.

11. This work was supported by the U.S. Army Research Office Contract No. DA AL03-87K-0057.

19 July 1988; accepted 12 August 1988

Dynamic Instability of Sheared Microtubules Observed by Quasi-Elastic Light Scattering

ROBERT A. B. KEATES* AND F. ROSS HALLETT

The kinetics of microtubule reassembly was studied in vitro by quasi-elastic light scattering (QELS). When microtubules assembled in the absence of microtubule-associated proteins (MAPs) were sheared, they rapidly depolymerized, recovered, and reassembled. The mean length of the recovered microtubules was the same as that observed just before shearing, implying that on average one fragment per original microtubule survived the fragmentation and recovery. When microtubules that contained 25 percent brain MAP were sheared, the fragments did not depolymerize extensively and the average length of the fragments decreased by a factor of 3 relative to the unsheared sample. The results support the dynamic instability model, which predicts that cellular microtubules are latently unstable structures protected on their ends by stabilizing caps.

THE DYNAMIC INSTABILITY HYPOTHESIS of microtubule assembly proposed by Mitchison and Kirschner (*1*) provides a ready explanation for many aspects of cell morphogenesis (*2*). We have adapted QELS to observe the dynamic instability of microtubules reassembled in vitro. The diffusive motions of microtubules in solution can be measured by QELS, from which the length distribution of a population can be calculated (*3, 4*). We observed clear evidence for dynamic instability in populations of microtubules, from their depolymerization and regrowth after shearing, in samples of microtubules assembled from purified tubulin, free of MAPs. The disassembly of the microtubules after shearing was consistent with the presence of protective caps at the ends of latently unstable polymers (*5, 6*). For microtubules that contained MAPs, we observed little depolymerization and regrowth of microtubules after shearing: the lack of depolymerization implied that MAP-containing microtubules were stable through most of their length.

Microtubules that are dynamically unstable should exist in two phases, one unstable and one stable. Rapid disassembly of the unstable population releases subunits that can contribute to the continued growth of

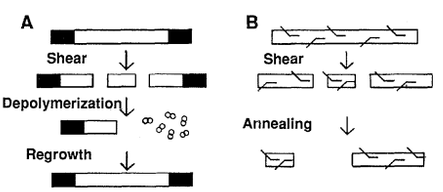

Fig. 1. Schematic outline of the experiments. In (**A**), MAP-free microtubules are shown terminated with protective caps that mask an unstable core. In the GTP-cap hypothesis, the caps contain tubulin-GTP, whereas the core is tubulin-GDP (*5*). When microtubules are fractured by shearing, uncapped fragments depolymerize rapidly, which releases tubulin subunits that can exchange GDP for GTP. The tubulin-GTP can then add to fragments that retain stable caps, allowing regrowth. In (**B**), MAPs bound to microtubules stabilize the polymer, so little depolymerization occurs on shearing and stable fragments are obtained. Over a period of time, some fragments may join and anneal, increasing the average length under steady-state conditions (*10*).

R. A. B. Keates, Biophysics Interdepartmental Group, Department of Chemistry and Biochemistry, University of Guelph, Guelph, Ontario, Canada N1G 2W1.
F. R. Hallett, Biophysics Interdepartmental Group, Department of Physics, University of Guelph, Guelph, Ontario, Canada N1G 2W1.

*To whom correspondence should be addressed.